npg

ORIGINAL ARTICLE

# A switch from hBrm to Brg1 at IFNγ-activated sequences mediates the activation of human genes

Yi Zhang[1, 2, *], Mo-bin Cheng[1, *], Yan-jun Zhang[1], Xin Zhong[1], Hui Dai[1], Li Yan[1], Ning-hua Wu[1], Ye Zhang[1], Yu-fei Shen[1]

[1]National Laboratory of Medical Molecular Biology, Department of Biochemistry and Molecular Biology, Institute of Basic Medical Sciences, Chinese Academy of Medical Sciences & Peking Union Medical College, 5 Dongdan Santiao, Beijing 100005, China

The SWI/SNF chromatin-remodeling complexes utilize energy from ATP hydrolysis to reposition nucleosomes and regulate the expression of human genes. Here, we studied the roles of human Brahma (hBrm) and Brahma-related gene 1 (Brg1), the ATPase subunits of the SWI/SNF complexes, in regulating human genes. Our results indicate that both hBrm and Brg1 interact with Signal transducer and activator of transcription (Stat) 1 *in vitro*. However, Stat1 in its native form only recruits hBrm to IFNγ-activated sequences (GAS) of individual genes; by contrast, in a stress-induced phosphorylated form, Stat1 mainly binds to Brg1. Under basal conditions, hBrm is recruited by native Stat1 to the GAS and exists in a mSin3/HDAC co-repressor complex on the *hsp90α* gene, which shows a compact chromatin structure. Upon heat-shock, hBrm is acetylated by p300 and dissociates from the co-repressor complex, which the phosphorylated Stat1 is increased, and binds and recruits Brg1 to the GAS, leading to elevated induction of the gene. This hBrm/Brg1 switch also occurs at the GAS of all of the three examined immune genes in heat-shocked cells; however, this switch only occurs in specific cell types upon exposure to IFNγ. Regardless of the stimulus, the hBrm/Brg1 switch at the GAS elicits an increase in gene activity. Our data are consistent with the hypothesis that the hBrm/Brg1 switch is an indicator of the responsiveness of a gene to heat-shock or IFNγ stimulation and may represent an "on-off switch" of gene expression *in vivo*.

## Introduction

Repositioning nucleosomes by ATP-dependent chromatin-remodeling complex is a classic example of chromatin remodeling that regulates eukaryotic genes *in vivo* [1-4]. SWI/SNF chromatin-remodeling complexes are conserved from yeast to humans. Human SWI/SNF are the homologs of the mating-type switching (SWI) and sucrose non-fermenting (SNF) complex in yeast and are named after their respective ATPase subunits:

Brahma-related gene 1 (Brg1) and human Brahma (hBrm) [5, 6]. The SWI/SNF complexes can activate or repress the transcription of their target genes [1, 7, 8].

Because Brg1 and hBrm are homologous, with 75% identity in amino-acid sequence, they are believed to have similar functions [9]. The two proteins, however, have distinct binding partners. The N-terminal domain of Brg1, for example, interacts with several zinc finger proteins, whereas hBrm interacts specifically with two ankryin-repeat proteins [10]. Brg1 and hBrm also have distinct but overlapping patterns of expression [11]. In mice, Brg1 is indispensable for embryonic development, and its loss causes embryonic lethality. *Brg1*-heterozygous mutant mice are susceptible to cancer, suggesting that it is a tumor suppressor [12]. Loss of hBrm, however, causes only limited defects in mice [1], and hBrm can compensate for the loss of Brg1 in Rb signaling, suggesting some overlapping functions [9, 13]. Recent reports with respect to many aspects of

development, cell growth and differentiation show that divergent functions of the SWI/SNF complexes depend on the ATPase subunits [7] and on the dynamic assembly of other subunits in a complex [14, 15].

These findings raise an interesting question: do Brg1 and hBrm function coordinately or divergently in response to environmental stresses, including non-lethal heat shock and IFNγ treatment? As ATP-dependent chromatin-remodeling complexes are non-specific for DNA binding, the specific DNA binding factors mediating their recruitment and function need to be identified first.

Signal transducer and activator of transcription (Stat) 1 functions as both a tumor suppressor and a direct mediator of IFNγ signaling. We have shown elsewhere that Stat1 enhances the promoter activity of the *hsp90β* gene under heat shock more efficiently than the traditional heat-shock factor (HSF) [16].

In this study, we explore the roles of the SWI/SNF chromatin-remodeling complexes in the expression and promoter activity of human genes in leukemic cell lines and primary T lymphocytes, where both Brg1 and hBrm are expressed. We first applied a non-lethal heat shock at 42 °C, and found that all of the genes examined were activated via hBrm-to-Brg1 switch at the IFNγ-activated sequences (GAS) in their promoters. This switch at GAS was mediated by Stat1, as Stat1 could interact with both hBrm and Brg1 physiologically. Heat-shock-induced phosphorylated Stat1 efficiently interacted with Brg1 but not with hBrm. Moreover, hBrm was acetylated by p300 upon heat shock, resulting in the release of hBrm from phosphorylated Stat1 at GAS and its subsequent replacement by Brg1. IFNγ also induced a similar hBrm-to-Brg1 switch via Stat1 at the GAS; however, this occurred only at selected IFNγ-induced genes in specific cell types.

## Results

### A switch from hBrm to Brg1 on the hsp90α promoter under heat shock

Stat1 is a key mediator of IFNγ signaling and directly regulates target gene expression in the nucleus through its binding to the GAS enhancer element [17-19]. We showed previously that Stat1 plays a pivotal role in regulating heat-shock-induced expression of *hsp90α* through its binding to the GAS site at the −1 612 to −1 605 position in the upstream promoter region [20]. Here, we further explored, with chromatin immunoprecipitation (ChIP) analysis, the involvement of the SWI/SNF complexes at the GAS region (−1 642/−1 485) of the *hsp90α* promoter before and after 30-60 min of heat shock at 42 °C (Figure 1A). Stat1 and hBrm occupied the GAS region at 37 °C, but hBrm was completely replaced

by Brg1 after 60 min of heat shock (H60). Brg1, along with Stat1, Stat3 and HSF1, occupied the GAS region at 42 °C. In addition, SNF5 (BAF47/Ini1), a core subunit shared by the SWI/SNF complexes, was also recruited to the *hsp90α* promoter both at 37 °C and under heat shock (Figure 1A).

To examine whether Brg1 and hBrm contribute to the regulation of *hsp90α* expression, we used RNA interference (RNAi) to individually knock down hBrm and Brg1 proteins in Jurkat cells. The respective small interfering RNAs (siRNAs) were able to efficiently knock down the relative levels of the proteins (Supplementary information, Figure S1a). Although none of the ATPases showed any impact on the basal expression of the *hsp90α* gene, the knockdown of Brg1, but not hBrm, significantly reduced the heat-shock activation of the gene by 67% (Figure 1B). This result suggests that while hBrm knockdown did not significantly affect the *hsp90α* gene activity in either case, the requirement of Brg1 is specific for the heat-shock-induced activity of the gene.

To further confirm the roles of Brg1 and hBrm, we examined the expression of a CAT reporter driven by an upstream, GAS-containing fragment (−1 756/+37 bp relative to the transcription start site) of the *hsp90α* gene in heat-shock response with a real time RT-PCR-based detection system (Figure 1C, top panel). The knockdown of either hBrm or Brg1 did not significantly affect the promoter activity at 37 °C. However, the knockdown of Brg1, but not hBrm, completely abolished the heat-shock induction of the activity of the hsp90α promoter (Figure 1C, bottom).

Unlike the mRNA profile (Figure 1B), the promoter activity of the *hsp90α* gene slightly increased in reporter assays of the two knockdown cells at 37 °C (Figure 1C, left panel), likely due to the lack of hBrm- or Brg1-regulated repressive element(s) beyond the −1 756/+37 promoter region of the *hsp90α* gene. While hBrm depletion did not change the promoter activities of *hsp90α*, either at 37 °C or under heat shock (Figure 1C, filled vs open bars), Brg1 knockdown specifically contributed to a 66% decrease in mRNA expression and promoter activity of *hsp90α* under heat shock (slashed bars).

The impact of hBrm or Brg1 knockdown on the promoter activity of the *hsp90α* gene with a wild-type GAS was as described above (Figure 1D, left panel, vs Figure 1C). However, this was not true when we used a mutant reporter construct (GXS) in which the first four base pairs of the GAS element (TTCCTACAA) were mutated (ccagTACAA; Figure 1D, central panel). GXS elicited much lower promoter activity under heat shock, which was insensitive to the knockdown of hBrm or Brg1
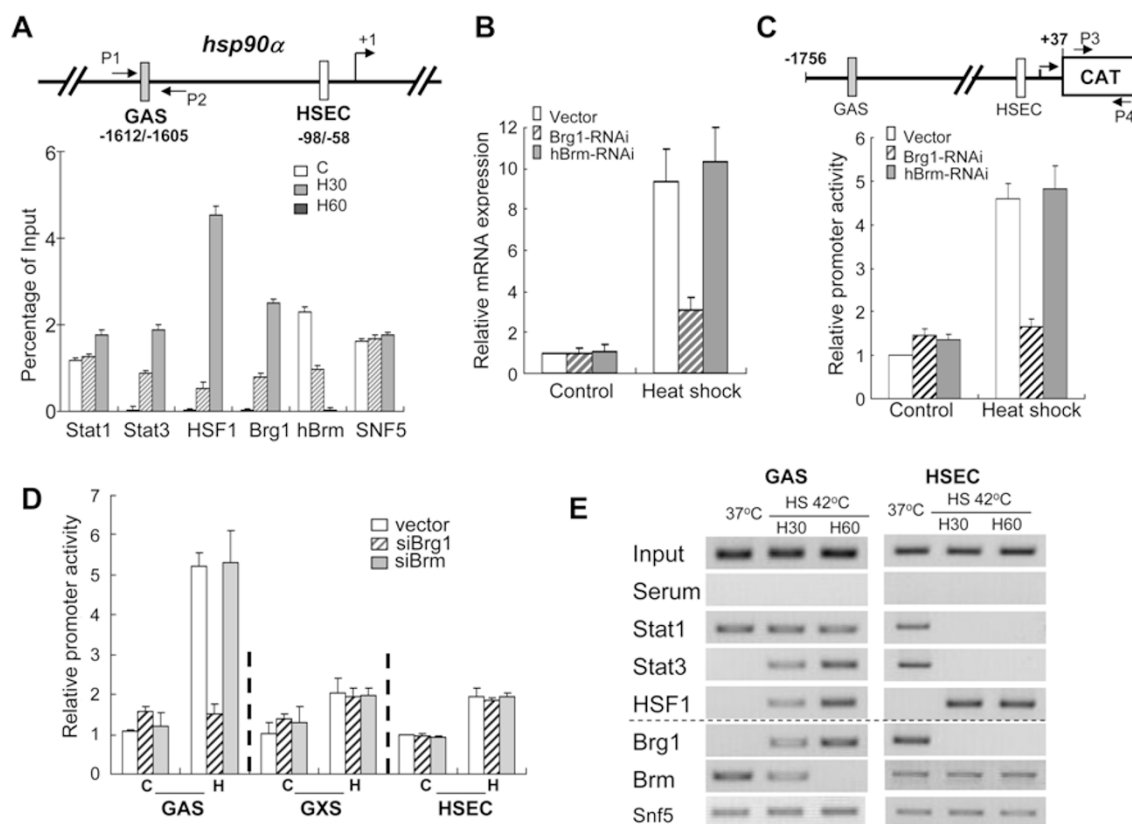
**Figure 1** Regulation of Brg1 and hBrm on *hsp90α* in a heat-shock response. **(A)** ChIP assays showing the recruitment of endogenous hBrm and Brg1 to the GAS of human *hsp90α*. Chromatin fragments pull-down immunoprecipitation (ChIP) was performed with antibodies for each factor, as indicated, and detected by qPCR analysis. H30: 42 °C for 30 min; H60: 42 °C for 60 min; C: 37 °C. Primers P1 and P2 amplify a GAS fragment spanning −1 642/−1 458 bp respective to the transcription initiation site at +1 of *hsp90α*. Each bar represents an average of at least three independent experiments, shown as the mean ± S.D. **(B)** Effects of siRNA specific for Brg1 or hBrm on the endogenous mRNA expression of *hsp90α*. Total RNA was extracted and quantified by qRT-PCR. **(C)** Effects of specific siRNA for Brg1 or hBrm on the promoter activity of *hsp90α* detected by qRT-PCR. The promoter activity was determined by the expression efficiency of a CAT reporter driven by a −1 756/+37 promoter fragment of *hsp90α* normalized to the expression of a co-transfected control of the pCCMV-*βGal* vector. Data are represented as the mean ± S.D. of three independent experiments. **(D)** Effect of hBrm and Brg1 on the promoter activities of *hsp90α* with wild-type GAS, mutant GXS and the proximal HSEC, GAS: TTCCTACAA, −1 756/+37; GXS: mutant GAS of ccagTACAA, −1 756/+37; HSEC: −125/+37 as the proximal promoter. Annotations as described for Figure 1C. **(E)** Electrophoretic profiles of the DNA products amplified in ChIP assay analysis at the GAS and a proximal element, HSEC element, of *hsp90α*. Antibodies used for ChIP analysis are shown on the left. Input: 5% of the DNA recovery from total chromatin fragments used as template and taken as 100%. Serum: negative control.

(Figure 1D, central panel), as was a proximal promoter construct designated HSEC (right panel). Because HSEC consists of Stat consensus elements that overlap with heat-shock elements (Supplementary information, Figure S1b), the HSEC sequences may provide a platform for recruiting HSF1 to substitute for Stat1 upon heat shock, as shown in the ChIP-agarose electrophoretic profile of HSEC (Figure 1E, right panel). Brg1 only associated with HSEC at 37 °C in the presence of Stat1 but not under heat shock. Throughout the heat-shock response, hBrm occupied the HSEC in a Stat1-independent manner. As

there was no correlation between Stat1 and the recruitment of hBrm or Brg1 in HSEC or other proximal regions of *hsp90α* gene (Supplementary information, Figure S1c), these data suggest that the two-fold increased promoter activity of HSEC upon heat shock (Figure 1D) was mediated by other factors, such as HSF1.

The above data reveal that only the GAS promoter but not the GXS or HSEC can mediate the hBrm- or Brg1-regulated efficient heat-shock induction of *hsp90α*. The GAS promoter-dependent *hsp90α* gene activity could thus be used as a model system to explore the

mechanisms of the regulation of human genes by hBrm and Brg1.

*Stat1 phosphorylation is necessary for it to interact with Brg1 under heat shock*

Despite reports indicating that Stat3 and Stat2 interact directly with Brg1 [21, 22], interactions between Stat1 and Brg1, and between any Stat family proteins and hBrm, especially under heat shock, remain unexplored. To examine these potential interactions directly, we generated HA-tagged, truncated forms of Stat1 (Figure 2A, S2-S6) and co-transfected the HA-tagged fragments of Stat1 with the respective ATPases into Jurkat cells.

Co-immunoprecipitation (co-IP) assays revealed that while the N-terminal domain (residues 1-136) of Stat1 was sufficient to interact with hBrm, its interaction with Brg1 required both the N-terminal and the coiled-coil

domains of Stat1 (residues 1-317) (Figure 2A, S3 & S4; Supplementary information, Figure S2b). The domain specificity of Stat1 for Brg1 binding at 37 °C was largely the same as reported for Stat2 [22], which required the N-terminal and the coiled-coil domain sequences in the relatively conserved regions of the two Stat proteins. However, the conserved phosphorylation sites in the C-terminal transactivation domain of Stat1 were unrelated to Brg1 binding (Figure 2A, S5 *vs* S2), similar to observations obtained for Stat3 [21].

We have previously shown that Stat1 is phosphorylated in heat-shocked cells [16, 20]; however, whether this is the key event in the subsequent recruitment of Brg1 upon heat shock at the GAS of the *hsp90α* gene remains unclear. Co-IP assays were used to determine the relative binding efficiency of Stat1 with the respective ATPases at 37 °C and after heat shock. Stat1 was efficiently co-
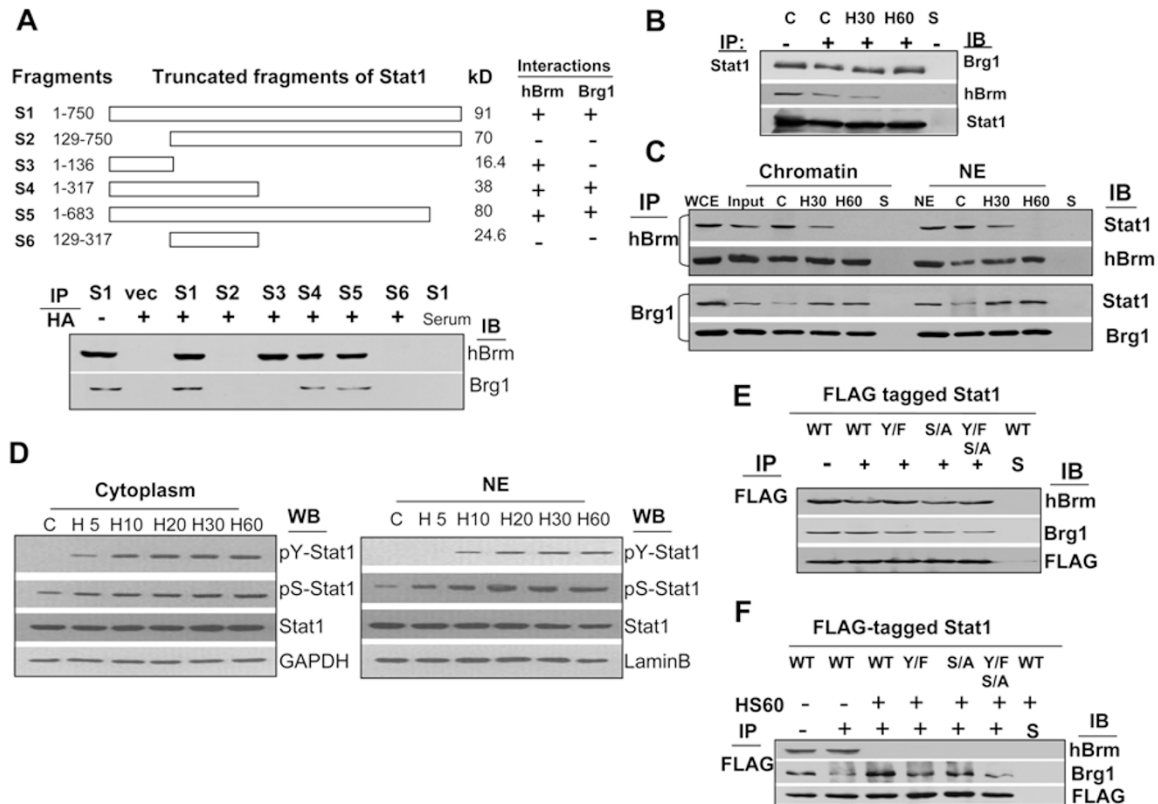


**Figure 2** Interactions of Stat1 with hBrm and Brg1. **(A)** Schematic drawing of the wild-type and truncated Stat1 fragments. "+" or "−": results of interactions between Stat1 (fragments) and hBrm or Brg1. Bottom panel: Co-IP assays with Jurkat cells transfected with HA-tagged Stat1 (S1-S6) or its vector, as control (vec). **(B)** co-IP of NE from Jurkat cells. IP: antibody used for immunoprecipitation; IB: antibodies used for immunoblotting; S: negative control; "+" or "−" indicates with or without IP. **(C)** Co-IP of proteins recovered from chromatin fragments and NE of Jurkat cells. Input: total chromatin fragments. **(D)** Western blot analysis of the cytoplasmic and nuclear fractions of Jurkat cells. pY-Stat1: phosphorylated Stat1 at Y701; pS-Stat1: phosphorylated Stat1 at S727; H5, H10, H20, H30 and H60: 42 °C for 5, 10, 20, 30 and 60 min, respectively. **(E, F)** Co-IP assays on FLAG-tagged mutants of Stat1 pre-transfected Jurkat cells. WT: wild-type Stat1; Y/F and S/A: Y701F- and S727A-Stat1; IP: antibody against FLAG; C: 37 °C; H: 42 °C for 60 min.

precipitated with hBrm at 37 °C. In contrast, Brg1 was preferentially bound to the presumably phosphorylated form of Stat1 after heat shock (Figure 2B and 2C).

Although the phosphorylation of both the Y701 (pY) and S727 (pS) residues of Stat1 was induced under heat shock, pS-Stat1 was seen even without heat shock (Figure 2D). However, pY-Stat1 was observed only in the cytoplasm of Jurkat cells 5 min after the initiation of heat shock and then in the nucleus at 10 min. This immediate induction of pY-Stat1 was likely catalyzed by a heat-shock-induced auto-activated Jak2 in the cytoplasm. Because the dominant-negative mutant of Jak2 failed to be activated via Y1007 phosphorylation (Supplementary information, Figure S2e and S2f), it also blocked the phosphorylation of Stat1 at Y701 in heat-shocked Jurkat cells (Supplementary information, Figure S2g). The role of Jak2 in phosphorylating pY-Stat1 was further confirmed in our recently published study on the regulation of *hsp90β* gene via an intronic heat-shock element [16].

To explore whether Stat1 phosphorylation enhances or interferes with the interactions between Stat1 and the ATPase subunits, we generated FLAG-tagged mutant forms of Stat1 carrying amino-acid substitutions of Y701F (Y/F) and S727A (S/A) either singly or in combination (Supplementary information, Data S1). The above amino-acid substitution mutants showed no effect on the binding between Stat1 and hBrm at 37 °C (Figure 2E); however, such substitutions, in particular the combination of both the Y/F and S/A mutations, markedly decreased the ability of Stat1 to bind to Brg1 under heat shock (Figure 2F). These data provide the first evidence that the C-terminal transactivation domain of Stat1 is pivotal in its preferential interaction with the SWI/SNF in the cellular stress response.

*Acetylation disrupts hBrm binding to Stat1 upon heat shock*

To examine whether Brg1 and hBrm modifications could affect their interaction with Stat1, we used a pan-specific antibody against acetyl-lysine to detect the potential acetylation of hBrm and Brg1. Our results revealed that hBrm, but not Brg1, was acetylated after 30 min of heat shock (Figure 3A). Heat shock also triggered an increase in the recruitment of histone acetyltransferases (HATs), including p300 and CBP, onto the *hsp90α* promoter, which was accompanied by elevated acetylation of H3K9 (lysine 9 of histone H3 (Figure 3B)). Co-IP experiments showed that hBrm existed in a complex containing CBP and p300, but not PCAF (Figure 3C), suggesting that CBP and p300 are likely responsible for the acetylation of hBrm upon heat

shock. Further studies with specific siRNAs for p300 and/or CBP showed that only the knockdown of p300 led to the retaining of hBrm at GAS, blocking the hBrm-to-Brg1 switch (Figure 3D) and reducing the promoter activity of the *hsp90α* gene under heat shock (Figure 3E). ChIP/ReChIP assays revealed that p300 was likely recruited to the promoter of heat-shock-activated genes via its direct interaction with phosphorylated Stat1 at GAS (Figure 3F).

We next examined whether acetylation could change the interaction between hBrm and Stat1 on the *hsp90α* promoter. We constructed FLAG-tagged mutants of hBrm with lysine-to-arginine mutations in the four consensus lysine residues in the C-terminal domain of hBrm (Figure 3G; Supplementary information, Data S1 and Figure S3a), as these sites were reported by Bourachot *et al.* [23] to be acetylation critical to Brm functions. The constructs with all four lysines mutated into arginines were designated Brm-R (Figure 3G, row 2). Those with only two residues mutated at a time were designated Bm-uR and Bm-dR (Figure 3G, third row and bottom row). We introduced the individual mutant constructs into Jurkat cells and used ChIP analysis to ascertain their binding efficiency at the *hsp90α* promoter. In contrast to the wild-type hBrm, which gradually reduced its binding to the GAS region on the *hsp90α* promoter over the course of the heat shock, Brm-R remained bound to GAS throughout the 60 min of heat shock (Figure 3H). The Bm-dR mutant, which contained the K1541R and K1543R mutations, behaved like the wild-type hBrm, whereas Bm-uR, with K1534R and K1535R mutations, behaved like Brm-R by remaining at the GAS under heat shock (Figure 3J). Moreover, Brm-R and Bm-uR efficiently reduced the promoter activity of *hsp90α* under heat shock, with no obvious effects on the basal activity at 37 °C (Figure 3K). These data suggest that acetylations at K1534 and K1535 likely mediate the heat-shock-dependent dissociation of hBrm from Stat1 at the GAS of the *hsp90α* gene.

Unlike the HATs that were recruited to the GAS and interacted with hBrm immediately after heat shock (Figure 3B and 3C), a mSin3a/HDAC repression complex was observed at the GAS of *hsp90α* gene along with hBrm and Stat1 at 37 °C (Figure 3L). mSin3a and HDAC2 within 30 min of heat shock, followed by a later dissociation of hBrm and HDAC1 from the GAS element as heat shock continued (Figure 3L). HDAC2 showed similar kinetics with mSin3A under heat shock and was thus likely the major HDAC subtype responsible for directing the repression complex to the *hsp90α* gene at 37 °C. These findings suggest that removal of the mSin3A/HDAC repression complex from the acetylated
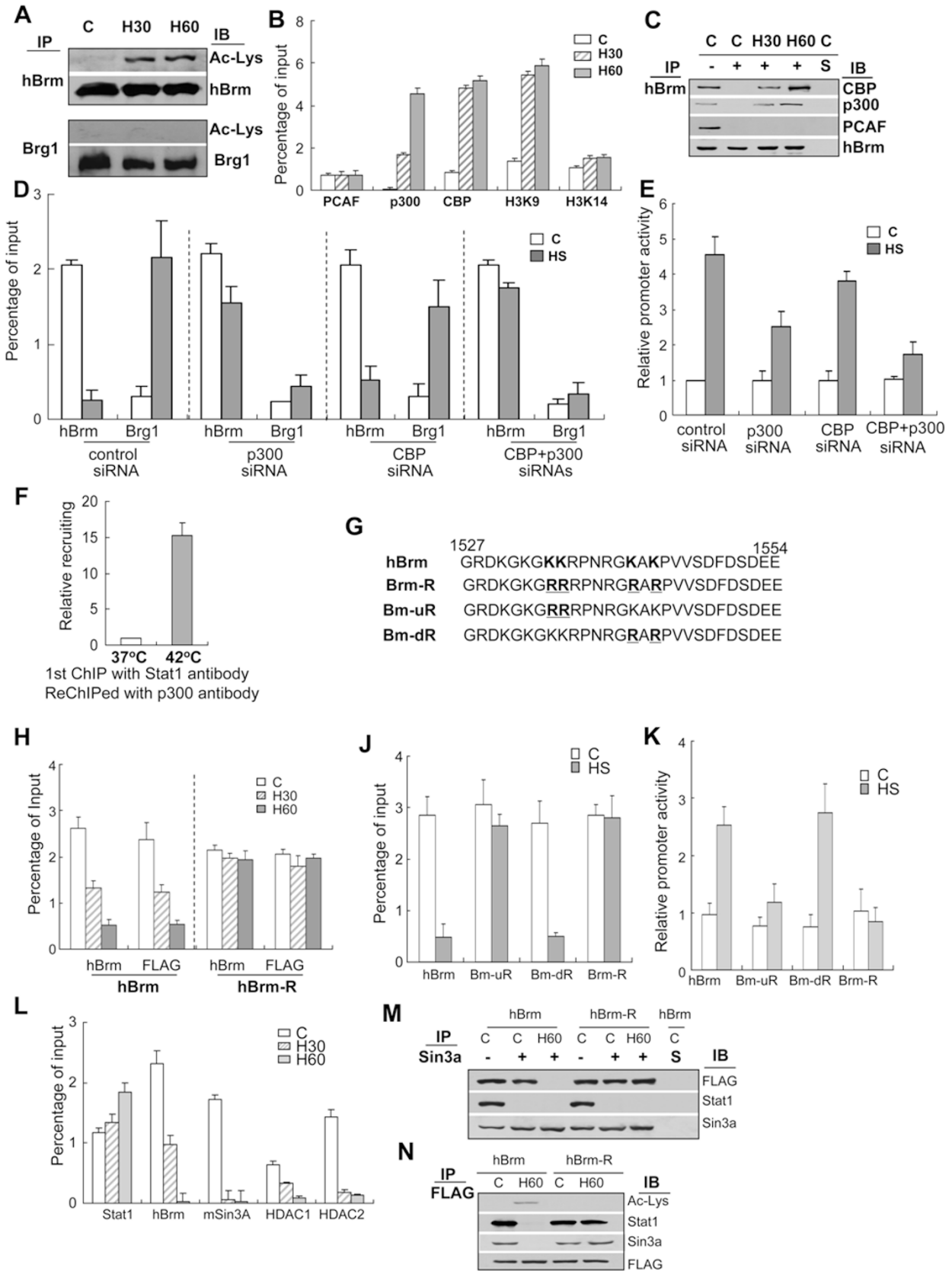
**Figure 3** hBrm acetylation and its interactions with HAT and mSin3a in regulating the promoter activity of *hsp90α*. **(A)** Co-IP analysis of Jurkat cell lysates to detect acetylation on the lysine residues of hBrm or Brg1. Ac-Lys: antibody against pan-acetyl-lysine. Other annotations as described in Figure 2B. **(B)** ChIP analysis examining the recruitment of endogenous PCAF, p300, CBP, H3K9ac and H3K14ac to the GAS site of *hsp90α*. Annotations as described for Figure 1A. **(C)** Co-IP assays detecting the interaction of hBrm with CBP, p300 and PCAF. **(D)** siRNA knockdown of p300, CBP and p300+CBP on the recruitment of endogenous hBrm and Brg1 at GAS of *hsp90α* in ChIP assays, with descriptions as in Figure 1A. **(E)** Impact of the transfected siRNAs on the promoter activity of *hsp90α*. Annotations as described for Figure 1C. **(F)** ChIP-ReChIP assay in Jurkat cells transfected with FLAG-tagged Stat1. Anti-FLAG was used for the first ChIP to recover Stat1-associated chromatin fragments at 37 °C and 42 °C. These fragments were then reChIPed at each of the previous temperatures with anti-p300. The relative recruitment of p300 at 37 °C and at 42 °C is shown in the histogram as mean ± S.D. **(G)** Protein sequences and positions of the K mutations in the C-terminus of hBrm. K (bold face): lysine residue to be mutated; hBrm: wild type; Brm-R: K to R mutation at all four residues; Bm-uR: only upstream two Ks mutated; Bm-dR: only downstream two Ks mutated. All mutated residues are in bold and underlined. Digits on top indicate the positions of amino acid residues. **(H, J)** Effects of the K/R mutations on the retention of hBrm at GAS upon heat shock, ChIP analysis of transfected Jurkat cells using FLAG-tagged hBrm, Brm-uR, Brm-dR and Brm-R. Antibodies against hBrm and FLAG were used for chromatin fragment pull down in parallel in **J** and FLAG alone in **H**. **(K)** Impact of the hBrm and mutation constructs on the promoter activity of *hsp90α*. Annotations as described for Figure 1C. **(L)** Recruitment of endogenous Stat1, hBrm, mSin3A and HDAC1/2 to the GAS as determined by ChIP analysis and as described for Figure 1A. **(M, N)** Co-IP assays to determine the interactions of wild-type and K/R-mutant hBrm with Sin3a and Stat1, respectively. Jurkat cells were transfected with either FLAG-tagged wild-type hBrm or FLAG-tagged Brm-R. Whole-cell extract used for IP with anti-mSin3A **(M)** and anti-FLAG **(N)**. Annotations as described for Figure 2E.

hBrm under heat shock is a prerequisite in the activation of *hsp90α* gene.

The above data indicate that a hBrm-mSin3a/HDAC complex occupies the GAS of *hsp90α* before heat shock, however, since mSin3a is unable to bind Stat1 (Figure 3M), the mSin3-HDAC co-repressor complex is likely recruited to the GAS via its interaction with hBrm. Thus, it appears necessary that the dissociation of ac-hBrm from Stat1 at GAS be preceded by the removal of mSin3a/HDAC co-repressor complex from hBrm upon heat shock (Figure 3L). Consistent with this hypothesis, the non-acetylated construct Brm-R, unlike the wild-type hBrm, did not dissociate from the mSin3a complex (Figure 3M and 3N) and remained on the *hsp90α* promoter under heat shock (Figure 3H and 3J). This was further confirmed with an *in vitro* pull-down experiment, which showed that the C-terminal residues 1 010-1 204 of mSin3a directly interact with wild-type hBrm, but not with its acetylated form (Supplementary information, Data S1, Table S7 and Figure S3b). These results indicate that the acetylation of hBrm determines the dissociation of hBrm from the Stat1/GAS complex and disrupts its interaction with the mSin3a complex.

*Stat1 mediates hBrm and Brg1 recruitment to the hsp90α promoter*

To examine whether Stat1 is critical in mediating Brg1 and hBrm recruitment to the GAS of *hsp90α*, we used an siRNA knockdown strategy to examine the interdependence of the players at this GAS. We first showed that the knockdown of either hBrm or Brg1 did not change the occupation of Stat1 at the GAS at 37 °C

and only modestly altered its binding under heat shock (Figure 4A-4C). Stat1 was constitutively bound to the GAS in the promoter of the *hsp90α* gene and did not require the presence of Brg1, as the binding was not blocked by Brg1 knockdown (Figure 4B). However, Stat1 knockdown abolished hBrm binding to the GAS, indicating that the recruitment of hBrm to the GAS was Stat1 dependent (Figure 4D; Supplementary information, Figure S4a). By contrast, a markedly higher recruitment of Brg1 was observed at the GAS upon heat shock when Stat1 was knocked down (Figure 4D), which suggests that certain secondary factor(s) could substitute for Stat1 under these conditions and could be responsible for this recruitment of Brg1 in heat-shocked cells.

To explore the insight therein, we next examined the effects of Stat3 and HSF1 knockdown on the recruitment of Brg1. We found similar recruitments of Stat1 and Brg1 at GAS in the knockdown cells as in the wild-type heat-shocked cells (Supplementary information, Figure S4b). Although Stat3 was unable to interact with Brg1 directly upon heat shock, HSF1 co-precipitated with Brg1 (Supplementary information, Figure S4c), suggesting that Stat3 may recruit Brg1 indirectly via HSF1 to the GAS upon heat shock. We then knocked down both Stat1 and Stat3 in Jurkat cells and found that, in addition to Stat1 and Stat3, the Brg1, HSF1 and hBrm recruitments to the GAS were all abolished (Figure 4E). As shown above, in the absence of Stat1, Brg1 was efficiently recruited to the GAS element of the *hsp90α* gene under heat shock, and this recruitment resulted in highly efficient promoter activity (Figure 4F and 4D). When Stat1 and Stat3 were both knocked down, the abnormally high promoter activ-
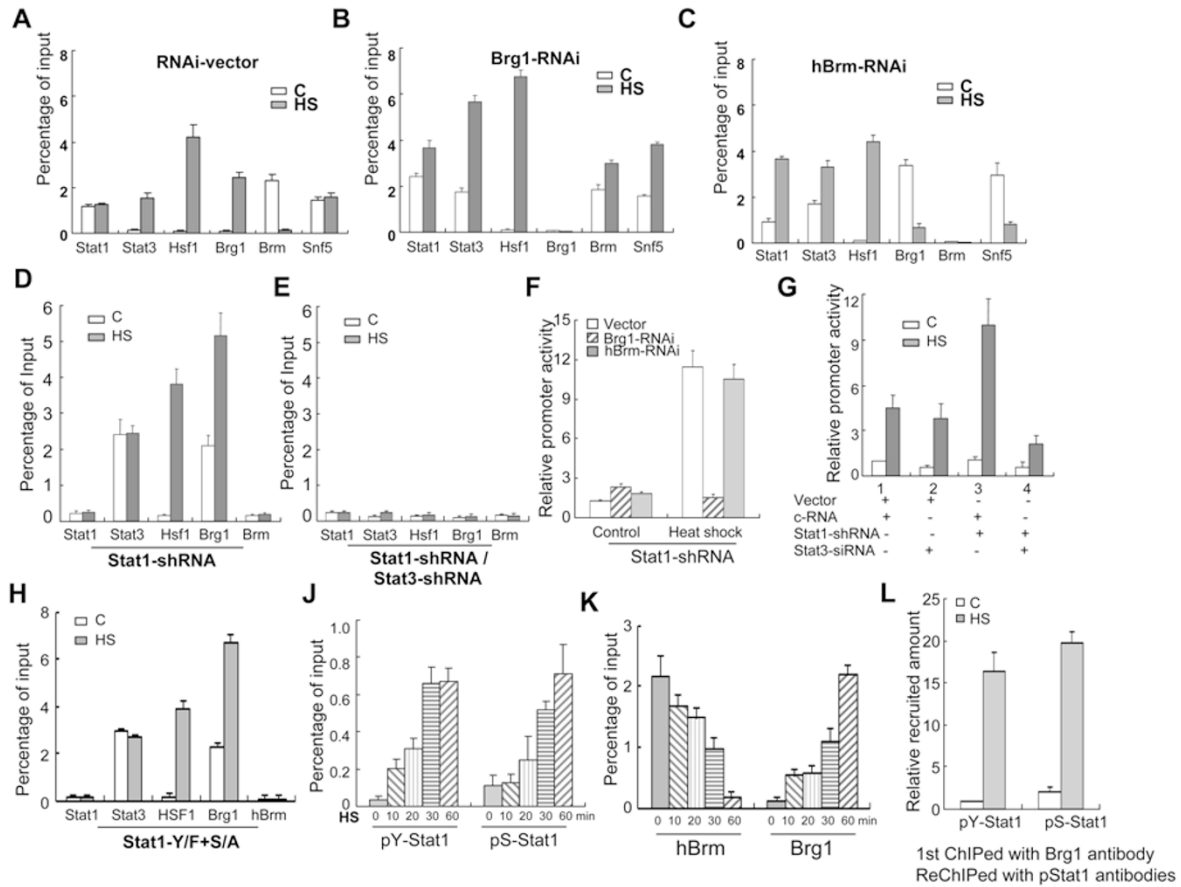
**Figure 4** Effects of Stat1 on promoting hBrm and Brg1 recruitment to the *hsp90α* GAS in a heat-shock response. **(A-D)** ChIP analysis of Jurkat cells transfected with vector and the respective siRNA for Brg1, hBrm and Stat1 to study their effects on recruiting endogenous factors to the GAS before and after heat shock. **(E)** ChIP analysis of Jurkat cells co-transfected with Stat1-siRNA and Stat3-siRNA. **(F)** Relative promoter activity of *hsp90α* in Jurkat cells with knockdown of Stat1, Brg1 or hBrm. Annotations as described for Figure 1C. **(G)** Relative *hsp90α* promoter activities with Stat1 and Stat3 knocked down individually or simultaneously in Jurkat cells. Vector: shRNA plasmid control for Stat1-shRNA; c-RNA: control RNA for Stat3-siRNA. Annotations as described for Figure 3E. **(H)** ChIP assay of Jurkat cells transfected with Stat1-Y/F+S/A double-mutant construct. Annotations as described for Figure 1A. **(J, K)** ChIP assays of pY-Stat1, pS-Stat1, hBrm and Brg1 at the *hsp90α* GAS. 0-60: incubation time in minutes at 42 °C. Each bar represents an average of at least three independent experiments and shows the mean ± S.D. **(L)** ChIP-ReChIP assay in Jurkat cells transfected with FLAG-tagged Brg1. Anti-FLAG antibody was used for the first ChIP to recover Brg1-associated chromatin fragments at 37 °C and 42 °C. These fragments were then ReChIPed at each of the previous temperatures with anti-pY-Stat1 and anti-pS-Stat1. The relative recruitment of pY-stat1 and pS-stat1 at 37 °C and at 42 °C is shown as the mean ± S.D.

ity in the absence of Stat1 (Figure 4F) was significantly reduced under heat shock (Figure 4G). These results suggest that Stat1 is a dominant factor in mediating Brg1 recruitment to the *hsp90α* GAS under heat shock and that Stat3 is a secondary factor that could mediate Brg1 recruitment in the absence of Stat1.

In addition to exploring the impact of phosphorylation on the recruitment of Stat1, we examined the binding efficiency of a dominant-negative mutant of Stat1 (Stat1-Y/F+S/A) at the GAS and found that the mutant Stat1 was unable to occupy the GAS (Figure 4H). This finding suggests that phosphorylation is critical for Stat1 to enter the nucleus and accumulate at the GAS. ChIP analysis further revealed that the abundance of Stat1 at the GAS was relatively stable throughout the 60-min heat shock (Supplementary information, Figure S4d). However, while pS-Stat1 was kept at a low level both before and throughout the first 10 min of heat shock, it gradually increased during the 60 min of heat shock. Similarly, little pY-Stat1 was bound to the GAS initially,

but increased binding was observed during the first 10-20 min and reached a plateau within 30 min of heat shock (Figure 4J). This result is consistent with the notion that heat shock induces Stat1 phosphorylation in the cytoplasm and enhances its distribution in the nucleus and its binding to chromatin. Additionally, the recruitment of phosphorylated Stat1 to replace its unphosphorylated form at the GAS is likely necessary for hBrm removal and Brg1 recruitment at the site upon heat shock (Figure 4K). With chromatin fragments first ChIPed with anti-FLAG antibody for Brg1-FLAG and then re-ChIPed with antibodies against pY-Stat1 and pS-Stat1, the ChIP-reChIP data revealed an at least 15-fold higher recruitment of phospho-Stat1 at the GAS upon heat shock than that at 37 °C (Figure 4L). These results indicate that phosphorylated Stat1 is necessary for the recruitment of Brg1 to the GAS to activate *hsp90α* gene

under heat shock.

A schematic representation of the hBrm-to-Brg1 switch at the GAS of *hsp90α* gene (Figure 5) shows the changes that occur during the transition from basal expression to an efficient induction of the *hsp90α* gene under heat shock. This model appears to hold for the role of the SWI/SNF chromatin-remodeling complexes in regulating human genes both under heat shock and in IFNγ induction, as indicated below.

### Heat-shock-induced hBrm-to-Brg1 switch in other GAS-containing genes and cell types

Because GAS elements are specific targets for IFNγ signaling in immune responses, we sought to determine whether other GAS-containing genes could be activated under heat shock via a similar hBrm/Brg1 switch at GAS. Indeed, in addition to *hsp90α*, heat-shock-induced
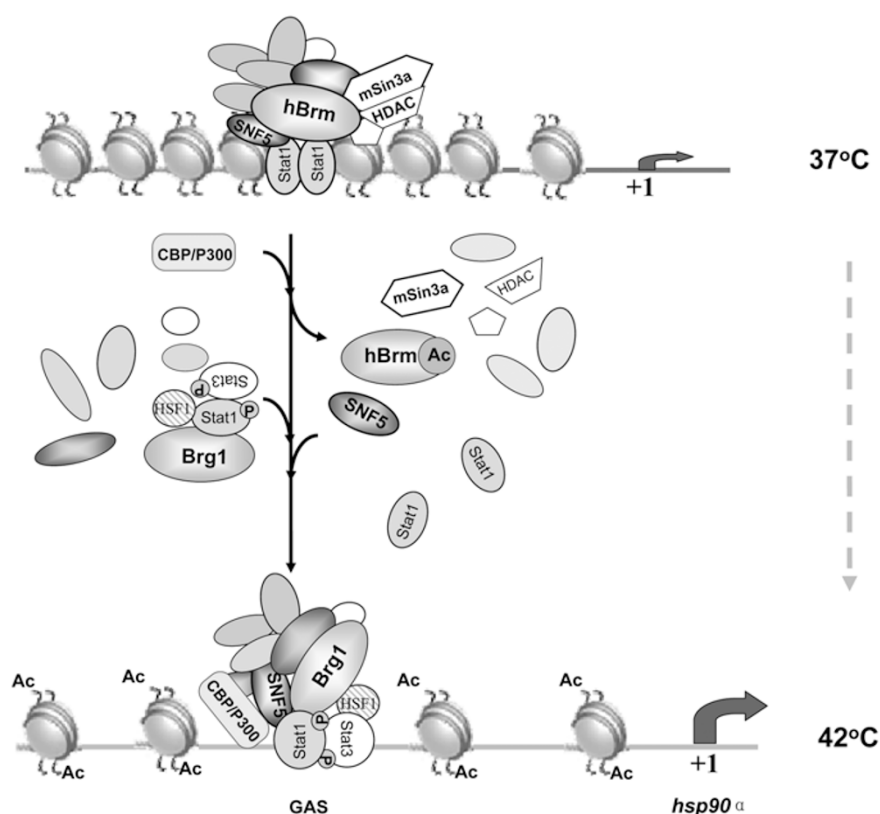


**Figure 5** Schematic representation of the hBrm-to-Brg1 switch at the *hsp90α* GAS after heat shock. **(A)** The physiological composition of the hBrm complex at the *hsp90α* GAS (top panel). CBP/p300-mediated acetylation of hBrm at the onset of heat shock, initiating the dissociation of hBrm from the mSin3A/HDAC co-repression complex, followed by the release of acetylated hBrm from the Stat1 complex at the GAS. **(B)** The switch of hBrm to the Brg1 complex at the GAS under heat shock (bottom panel). Phosphorylated Stat1 induced upon heat shock forms a heterotrimer with Stat3 followed by HSF1 that is responsible for the recruitment of the Brg1 complex to the GAS. The Brg1 complex and acetylated H3K9 mediate an open conformation of chromatin surrounding the GAS promoter and enhances the heat-shock induction of the *hsp90α* gene (heavy arrow).

expression of *CIITA*, *BCL6* (Figure 6A, open bars) and *IRF-1* in Jurkat cells (Supplementary information, Figure S5a, left panel), and *hsp90α*, *CIITA* and *BCL6* in heat-shocked Raji cells (Figure 6B) was observed. The effects of heat-shock induction on these genes were mainly regulated by Brg1, similar to the response of the *hsp90α* gene in Jurkat cells (Figure 1B). Further analyses revealed that these genes were likely activated via a Stat1-mediated hBrm-to-Brg1 switch on their GAS elements (Supplementary information, Table S4), such as the non-translated first exon of *BCL6* in Jurkat cells (Figure 6C), promoter IV of *CIITA* in Raji cells (Figure 6D), and the upstream of *IRF-1* (Supplementary information, Figure S5a) in Jurkat cells with heat-shock induction. As Jurkat cells are derived from human leukemic T cells, determining whether the heat-shock-induced hBrm-to-Brg1 model established from tumor cell lines can be validated in human primary cells is of great importance. We examined the enriched T lymphocytes from human peripheral blood and confirmed the heat-shock-induced elevated expression of the *hsp90α* gene and a Stat1-mediated hBrm-to-Brg1 switch at the GAS region of

the gene in these primary T cells (Supplementary information, Figure S5b), similar to that shown in the heat-shocked Jurkat cells (Figures 1B and 6C, left panel).

Using the *BCL6* gene as a model in heat-shocked Jurkat cells, we observed a novel result: the Brg1 recruitment to the *BCL6* GAS was Stat1 dependent. This result is straightforward, because Stat3, which co-existed with Stat1 at the *hsp90α* gene, was not present in the heat-shock complex at this GAS, and the knockdown of Stat1 completely abolished the recruitment of Brg1 to the *BCL6* GAS (Supplementary information, Figure S5c).

### IFNγ-induced hBrm-to-Brg1 switch at GAS is cell type specific

In contrast to the results with heat shock, IFNγ treatment showed cell type specificity in its effects on gene expression. Specifically, it only induced the expression of *BCL6* and *IRF-1,* but not *hsp90α* and *CIITA*, in Jurkat cells (Figure 7A, left panel; Supplementary information, Figure S5a, right panel). In Raji cells, only increased *CIITA* expression was observed (Figure 7A, right panel). IFNγ also induced a hBrm-to-
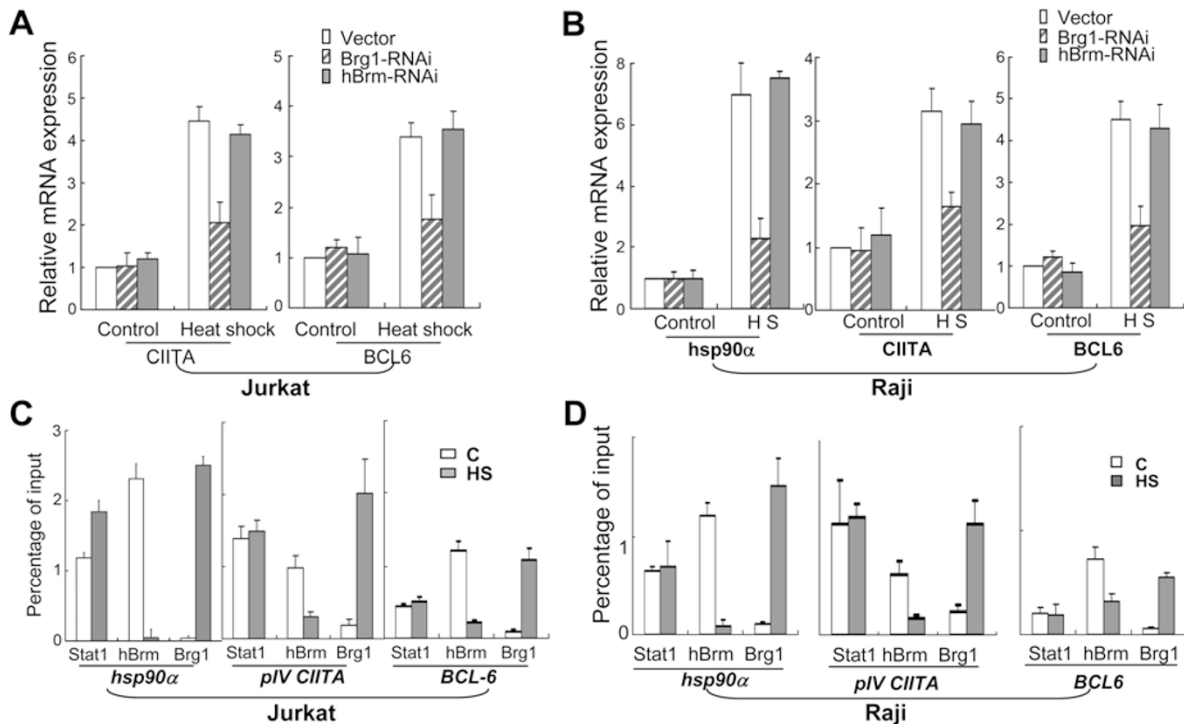


**Figure 6** The hBrm-to-Brg1 switch at the respective GAS elements of *hsp90α*, *CIITA* and *BCL6* and the activation of specific genes in Jurkat and Raji cells upon heat shock. **(A**, **B)** Effects of siRNA specific for Brg1 or hBrm on the endogenous mRNA expression of *CIITA* and *BCL*6 in Jurkat **(A)** and of *hsp90α* in Raji **(B)** cells. Total RNA was extracted and quantified by qRT-PCR. **(C**, **D)** ChIP analysis showing the recruitment of endogenous Stat1, hBrm and Brg1 at the respective GAS regions of the *hsp90α*, *pIV-CIITA* and *BCL6* genes in Jurkat **(C)** and Raji **(D)** cells.
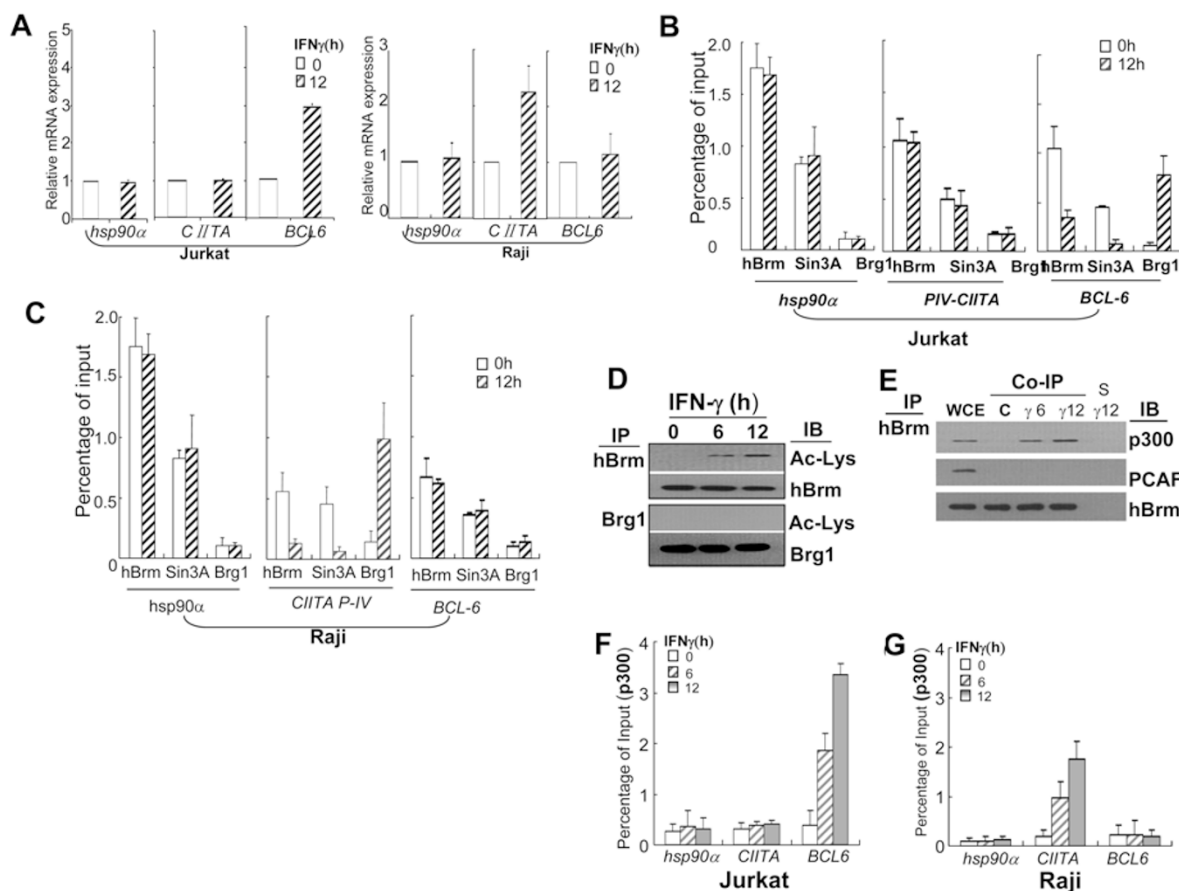
**Figure 7** The hBrm-to-Brg1 switch at the respective GAS elements of the *hsp90α*, *CIITA* and *BCL6* genes and the activation of the genes in Jurkat and Raji cells upon IFNγ treatment. **(A)** Effects of IFNγ on the endogenous mRNA expression of *hsp90α*, *CIITA* and *BCL-6* in Jurkat or Raji cells with or without IFNγ treatment for 12 h. **(B, C)** ChIP analysis demonstrating recruitment of hBrm, mSin3A and Brg1 to the respective GAS of the *hsp90α*, *p-IV CIITA* and *BCL6* genes in the genomes of Jurkat **(B)** and Raji **(C)** cells after IFNγ treatment (1 μm, 12 h). **(D)** Co-IP analysis of the Jurkat cell lysates to detect the acetylation of the lysine residues of hBrm or Brg1 under IFNγ treatment. Ac-Lys: antibody against pan-acetyl-lysine. 0, 6, 12 h of IFNγ treatment. **(E)** Co-IP assays detecting the interaction of hBrm with p300 and PCAF with IFNγ treatment. Annotations as described in **(D)**. **(F, G)** ChIP analysis demonstrating the effect IFNγ treatment on the recruitment of endogenous p300 to the respective GAS regions of the *hsp90α*, *pIV-CIITA* and *BCL-6* genes in Jurkat **(F)** and Raji **(G)** cells.

Brg1 switch at the GAS of the activated genes in each of the cell types (Figure 7B and 7C). Moreover, while the mSin3A repression complex occupied the GAS of all of the genes examined in both cell types, only the two IFNγ-activated genes showed a depletion of the mSin3A complex simultaneously with the reduction of hBrm at the GAS and recruitment of Brg1 during IFNγ treatment (Figure 7B, right and Figure 7C, middle panels). In contrast to Jurkat cells, *CIITA* responded to IFNγ in Raji cells, as reported in a study by Holling *et al.* [24]. Therefore, it was not surprising that the GAS in promoter IV of the *CIITA* gene showed a switch from hBrm to Brg1 after treatment with IFNγ (Figure 7C, middle). Thus, a hBrm-to-Brg1 switch at GAS along with mSin3A depletion

indicates a successful induction of these on the genes by INFγ.

Similar to the heat-shock response, IFNγ treatment induced acetylation of hBrm, but not Brg1 (Figure 7D). Consistent with this finding, hBrm was associated with a complex containing p300 (Figure 7E) in Jurkat cells. Although p300 recruitment was enhanced under heat shock in all of the genes examined (Supplementary information, Figure S6), upon INFγ treatment, it accumulated specifically at the *BCL6* GAS in Jurkat cells (Figure 7F) and at the GAS of pIV of *CIITA* in Raji cells (Figure 7G). Thus, similar to its role under heat shock, p300 appears also critical in IFNγ signaling and is likely recruited by the phosphorylated Stat1, as shown under heat shock

(Figure 3F).

### hBrm-to-Brg1 switch induces chromatin conformational changes

To explore whether the switch from hBrm to Brg1 at GAS is correlated with an open and active conformation of chromatin in gene promoters, restriction endonuclease accessibility assays were performed. The accessibility of endonuclease *Apa*I on the GAS region of *hsp90α* (Figure 8A), of *Pst*I on that of the *CIITA p*IV (Figure 8D) and of *Sac*I on that of *BCL6* (Figure 8G) was examined. The GAS region of *hsp90α* became accessible to *Apa*I only under heat shock in Jurkat and Raji cells, with a ~50% *Apa*I digestion upon heat shock (Figure 8B and 8C, filled bars). The *Pst*I profiles of *CIITA* in heat-shocked or IFNγ-treated Jurkat cells (Figure 8E) were comparable to those performed with *Apa*I on the *hsp90α* GAS. However, as *CIITA* is expressed in antigen-presenting cells, including B-cell-derived cells like Raji [24], the pIV could thus be exposed to *Pst*I without any treatment, resulting in a ~50% digestion of the fragments with *Pst*I (Figure 8F, open bars). Further treatment of Raji cells with heat shock (Figure 8F, left) or IFNγ (Figure 8F, right) led to 85% of the promoter fragments being ultimately digested. The *Sac*I digestion patterns of *BCL6* under heat shock and IFNγ treatment in Jurkat cells were comparable to that of *CIITA* digestion with *Pst*I in the Raji cells (Figure 8H and 8F). These data indicate that the IFNγ-induced hBrm-to-Brg1 switch directed the formation of an open and transcriptionally active chromatin conformation at the promoter of *CIITA* in the Raji cells and at the GAS of *BCL6* in Jurkat cells.
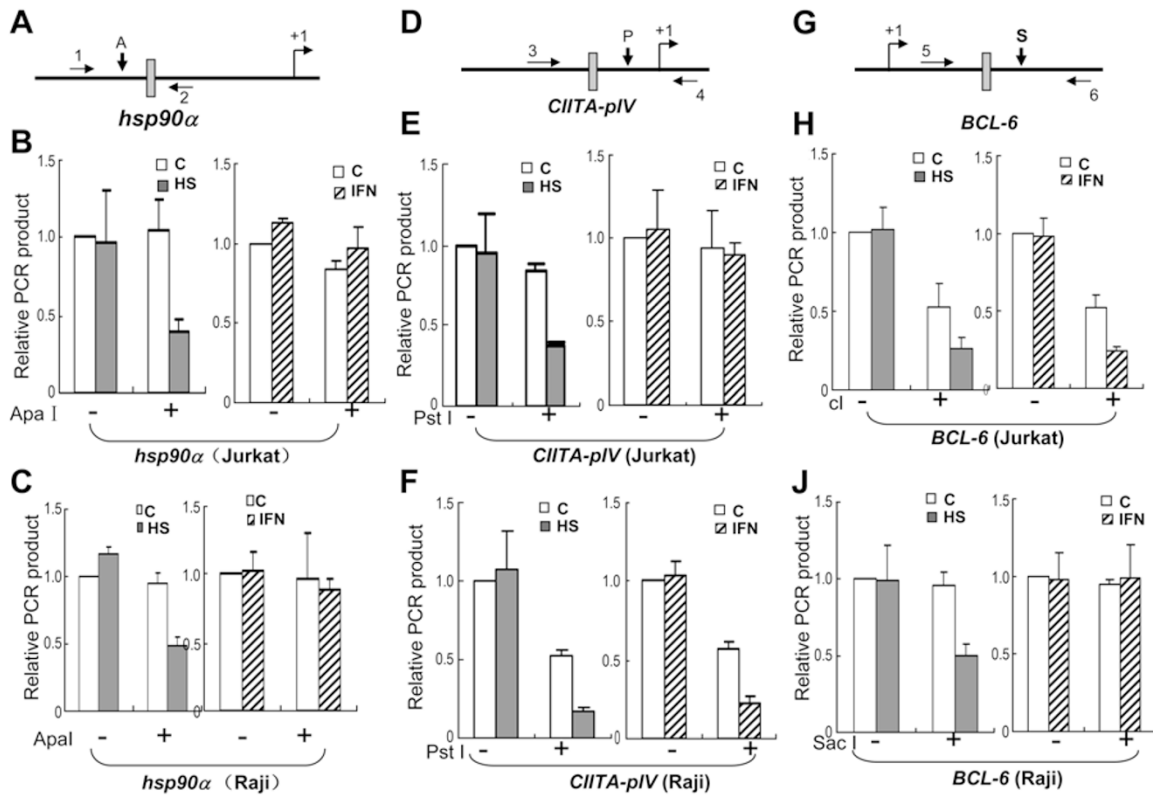


**Figure 8** The hBrm-to-Brg1 switch induces chromatin conformational changes. **(A)** Schematic representation of the positions of the cutting site of the restriction endonuclease *Apa*I (A) and the primer pairs relative to the *hsp90α* GAS. +1: transcription initiation site; +: endonuclease applied. **(B, C)** Accessibility of *Apa*I at the *hsp90α* GAS was elevated upon heat shock, but not on IFNγ treatment, in Jurkat and Raji cells, respectively. **(D)** Schematic representation of the positions of the cutting site of the restriction endonuclease *Pst*I (P) and the primer pairs relative to the *pIV-CIITA* GAS. **(E)** Accessibility of *Pst*I at the *CIITA* GAS was elevated upon heat shock, but not on IFNγ treatment, in Jurkat cells. **(F)** The *pIV-CIITA* gene was in an open conformation and was further induced upon heat shock or IFNγ treatment in Raji cells. **(G)** Schematic representation of the positions of the cutting site of the restriction endonuclease *Sac*I (S) and the primer pairs relative to the *BCL6* GAS. **(H)** The *BCL6* gene was in an open conformation and was further induced upon heat shock or IFNγ treatment in Jurkat cells. **(J)** Accessibility of *Sac*I at the *BCL6* GAS was elevated upon heat shock, but not on IFNγ treatment, in Raji cells.

## Discussion

Recent evidence demonstrates that the SWI/SNF chromatin-remodeling complexes can be tailored for appropriate functions in stage-specific gene expression in neural development. This can be achieved by either exchanging the subunit components or substitution between the homologous members of the complexes [25, 26]. During osteoblast development, the SWI/SNF complexes can bind distinct elements to determine the stage-specific expression of a gene [7]. However, how SWI/SNF chromatin-remodeling complexes work in human cells under environmental stress is largely unknown.

On this specific topic, our findings show that the exchange of the ATPase subunits of the SWI/SNF chromatin-remodeling complexes from hBrm to Brg1 at the specific GAS element enables human genes to be activated in response to heat shock or IFNγ treatment. Here, we have demonstrated, in three GAS-containing genes in two leukemic cell lines and primary T cells from human periphery blood (Supplementary information, Figure S5b), that hBrm acetylation and the phosphorylation of Stat1 are essential for the hBrm-to-Brg1 switch to occur at the GAS to activate the stress-induced response.

We suggest that post-translational modifications of hBrm and Stat1 are critical for the hBrm-to-Brg1 switch. First, the hBrm in the mSin3a co-repressor complex can stably interact with Stat1 and occupies the GAS promoter; however, once acetylated, hBrm can no longer bind the mSin3a complex or Stat1, which results in the breakdown of the repression complex and removal of hBrm. It appears from our results that the HAT p300 is activated and acetylates hBrm in all of the heat-shocked cells examined; however, p300 is recruited to a limited number of GAS sites in the genes that preferentially respond to IFNγ treatment in these cells (Figure 7F-7G). Heat shock can induce an immediate elevation in tyrosine phosphorylation of Stat1, which then enters the nucleus and binds to GAS in promoters as soon as the hBrm complex is evacuated. At the GAS, pS-Stat1 exists at minimal levels and is induced, along with pY-Stat1, to fully occupy the GAS of the genes upon heat shock. Brg1 is concurrently recruited to the GAS to elicit an open chromatin conformation for the activation of the genes.

The fact that Stat1 without Y701 phosphorylation can dimerize in a parallel conformation via its N-terminal domain and enter the nucleus before activation [27, 28] could explain the constant level of Stat1 constitutively bound to GAS before stimulation and under heat shock (Supplementary information, Figure S4d). At the onset of heat shock, while pS increases gradually, pY-Stat1 in-creases immediately and reaches a plateau within 30 min. The elevated level of pY-Stat1 can facilitate heterodimer formation with Stat3, and the resulting heterodimer can presumably enter the nucleus and substitute for the non-phosphorylated Stat1 at GAS upon heat shock.

Stat1 is pivotal in the hBrm-to-Brg1 switch at the specific GAS in all of the genes examined. It facilitates the recruitment of hBrm under basal physiological conditions, which then dissociates in its acetylated form upon heat shock. Although the determinant role of Stat1 on Brg1 recruitment upon heat shock is not straightforward, the data indicate that Brg1 recruitment is also Stat1 dependent. While knockdown of Stat3 does not significantly change the profiles of Stat1 and Brg1 at GAS under heat shock (Supplementary information, Figure S4b), co-knockdown of both Stat1 and Stat3 completely abolishes the heat-shock-induced recruitment of Brg1 and HSF1 (Figure 4F). It is likely that, in the absence of Stat1, Stat3 can recruit HSF1 that further interacts with Brg1 [29] resulting in an over-recruitment of Brg1 to GAS (Figure 4D) and an inappropriately high induction of the *hsp90α* gene (Figure 4F). Stat3 activation is greater and more prolonged in tumor cells than in wild-type cells, in the absence of Stat1 [30]. Whether this is a general feature of the oncogene Stat3 that is otherwise counteracted by the tumor suppressor Stat1 when both are expressed is not known [31]. Due to the lack of Stat3 at the *BCL6* GAS, the recruitment of Brg1 and hBrm at this GAS promoter is abolished in Stat1-knockdown cells upon heat shock, and thus the expression of the *BCL6* gene is reduced (Supplementary information, Figure S5c).

The presence of HDACs in the mSin3/HDAC co-repressor complex is evolutionarily conserved from yeast to mammals. Mammalian Sin3a is a co-repressor complex with at least eight core subunits [32, 33]. Recent studies show that regulatory proteins, including DNA-binding proteins, transiently associated with the mSin3 complex can turn this complex into either a repressor or an activator of transcription. However, if this complex is not tethered to a proximal promoter, no impact on transcriptional regulation is observed [33, 34]. As hBrm knockdown does not obviously affect *hsp90α* promoter activity at 37 °C (Figure 1C), it is likely that hBrm recruits mSin3a to the GAS via a direct interaction (Supplementary information, Figure S3b) to form a compact chromatin structure without activation of the gene. It is also likely that HDAC1/2 in the mSin3 repressor complex with hBrm1 at the *hsp90α* GAS prohibits H3K9 and hBrm from being acetylated and stabilizes the hBrm complex before heat shock [35]. By contrast, at the onset of heat shock or IFNγ treatment, pY-Stat1 and pS-Stat1 recruit p300/CBP to the GAS (Figure 4L). p300/CBP

acetylates H3K9 to elicit an active chromatin signal, and the hBrm to initiate the switch at the GAS. As heat shock continues, phosphorylated Stat1 substitutes for the non-modified Stat1 at the GAS (Figure 4J), recruits the Brg1 chromatin-remodeling complex to the GAS promoter and induces appropriate promoter activity of the gene (Figure 1C, open bars). The hBrm-to-Brg1 switch provides an open chromatin conformation that facilitates the activation of human genes under heat shock or IFNγ signaling.

SNF5 (Baf47/Ini1) is a core subunit of the mammalian SWI/SNF chromatin remodeling complexes [36, 37], and it is a tumor suppressor that plays important roles in cellular differentiation and development [5]. In hBrm- or Brg1-knockdown cells, SNF5 recruitment was at a similar level as the ATPase subunit that remained at the promoter either at 37 °C or 42 °C (Figure 4A-4C), which suggests that SNF5 is required to work together with the ATPase available at GAS throughout the heat-shock response. The overexpressed core components of the BAF complex can be sequentially assembled on its target DNA element in certain viral infected cells. In this model, Brg1 arrives at the target site within 10 min after the infection, but the other components are not observed until 90 min later [38, 39]. If this can be validated *in vivo*, it would suggest that SNF5 may function as a platform to facilitate the switch of the chromatin remodeling complexes by forming a complex with hBrm without heat shock, but docking Brg1 instead immediately after heat shock.

It is worth noting that we have observed this hBrm-to-Brg1 switch in several human genes under heat shock and/or IFNγ treatment, suggesting that this, or a similar switch, is likely used by many other genes under physiological and pathological conditions. In addition, this hBrm-to-Brg1 switch at the GAS enhancer could also serve as an indicator of whether a gene is efficiently responsive to heat shock and/or IFNγ, which may be explored to manipulate the expression of otherwise silenced immune genes in response to external stress or stimulus.

## Materials and Methods

### Plasmids and siRNA

Expression plasmids of wild-type Stat1 (pSG91) and mutant Stat1 (Y701F) were from Dr XY Fu (Indiana University). The Stat1 S727A plasmid was from Dr CM Horvath (Mount Sinai School of Medicine). The pBS(KS+)CehBRM plasmid was from Dr AN Imbalzano (University of Massachusetts). The −1 756/+37 fragment of the *hsp90α* gene was inserted into the pREP4m/CAT reporter plasmid mutated from pREP4/CAT (Invitrogen, Carlsbad, CA, USA) and used to detect the promoter activity of the gene. The transfection control plasmid pCMV-β-gal was constructed as described previously [40]. Small hairpin RNA (shRNA) constructs

against Stat1 were from Origene Technologies, Inc (Rockville, MD, USA). Commercialized p300-siRNA, CBP-siRNA and Stat3-siRNA were from RiboBio Co, Ltd (Guangzhou).

### Antibodies

Anti-HSF1 was obtained from Dr S Calderwood (Harvard Medical School). Antibodies against Stat1, Snf5, Brg1, hBrm, p300, CBP, mSin3A, PCAF, Stat3, HA and Protein A (or G)-agarose were purchased from Santa Cruz Biotechnology (Santa Cruz, CA, USA). Anti-FLAG (M2) antibody was from Sigma-Aldrich Co (St Louis, MO), and anti-pan-acetyl-lysine, Ac-H3K9 and Ac-H3K14 were from Upstate Biotechnology (Syracuse, NY, USA).

### Cell culture and treatments

Jurkat and Raji cells were cultured as instructed by ATCC. Heat shock was carried out at 42 °C for 60 min or as indicated. In all, 1 nM IFNγ (Repro Tech Inc, Rocky Hill, NJ, USA) was used to treat the cells for 12 h. For kinetic studies, cells were assayed at 6 h intervals from 0-24 h.

### Recombinant DNA constructs

The procedures for the construction of the following are described in Supplementary information, Data S1: Brg1-RNAi and hBrm-RNAi (Supplementary information, Table S1); truncation mutants of Stat1 (Supplementary information, Table S2); and construction of K/R mutations in the C-terminal of hBrm (Supplementary information, Table S3).

### DNA transfection and promoter activity assay

Transfections were carried out using electroporation (Gene Pulser II, Bio-Rad). Cells were transfected with RNAi, truncated constructs or mutant constructs and were allowed to recover for 48 h prior to promoter activity analysis. For promoter activity analysis, each CAT reporter plasmid was mixed with the control plasmid pRC-CMV-βGal at an appropriate molar ratio and were co-transfected into host cells at $2 \times 10^7$. At 48 h post-transfection, total RNA was extracted and CAT mRNA levels were determined by quantitative real-time RT-PCR [40]. To detect the induction of the CAT reporter, the following primers were used: for the CAT promoter, forward primer 5′-ACTTCTTCGCCCCCGT-3′ and reverse primer 5′-CCGCCCTGCCACTCAT-3′; and for the control plasmid of pCMV-β-*gal*, forward primer 5′-CTTACGGCGGTGATTTTGG-3′ and reverse primer 5′-TGCTGCTGGTGTTTTGCTT-3′. The cycle number required to reach a threshold in the linear range (Qt) was determined and compared with a standard curve for each primer set generated by five five-fold dilutions of the first-strand cDNA of known concentrations. Data represent the mean ± S.D. of normalized CAT promoter relative to that of pCMV-β-*gal.* The shRNA constructs from Origen were incubated for 72 h post-electroporation before harvesting as recommended by the provider. For knockdown of p300, CBP or Stat3, 100 nM (final concentration) of the respective siRNA was used for transfection.

### Immunoprecipitation and immunoblot analyses

Whole-cell extracts or nuclear extracts (NE) were prepared as previously described [41]. Co-IP analyses were performed with ~500 μg of proteins incubated with specific antibodies for 2 h at 4 °C. In all, 20 μl of Protein A (or G)-agarose was added and

incubated at 4 °C overnight. Pellets were then washed with RIPA buffer, followed by addition of 40 µl of 1× Laemmli buffer, and then they were suspended and boiled. Samples were separated by SDS-PAGE and analyzed by western blotting sequentially with individual antibodies [26].

*ChIP and qPCR analyses*

Cultured cells and peripheral blood-enriched T lymphocytes were treated without or with heat shock or interferon treatment. ChIP analyses were then carried out with formalin cross-linking as previously described [20, 42]. For quantitative analysis, standard curves and ChIPed DNA samples were analyzed on a Rotor-Gene RG-3000A Real-Time PCR System (Corbett Research, Australia) with PCR Master Mix for SYBR Green assays (TaKaRa, Biotech). The cycle number required to reach a threshold in the linear range (Qt) was determined and compared with a standard curve for the primer set generated by five 10-fold dilutions of genomic DNA samples of known concentrations. Amplified products were separated on a 1.5% agarose gel and visualized by ethidium bromide staining. Gel images were scanned with an AlphaImager 2000, as described previously [43]. In all the experiments, following cycling parameters were used: 95 °C for 10 s and 40 cycles of 95 °C for 10 s, 60 °C for 10 s and 72 °C for 10 s. The percentage of ChIPed DNA relative to input was calculated and is shown as mean value ± S.D. from three independent experiments.

To detect the proteins from chromatin fragments ChIP was first carried out to obtain specific chromatin fragments that were incubated at 65 °C for 4 h to reverse the cross-linked protein-DNA complex and release the proteins. Specific proteins were then eluted from Protein A (or G) beads and subjected to standard procedures for western blot analysis.

Primer sets used in ChIP assays for individual GAS in the promoters of *hsp90α*, *CIITA*, *BCL6* and *IRF1* are described in Supplementary information, Table S4.

For ChIP-reChIP analysis [44], Jurkat cells were first transiently transfected with FLAG-tagged Brg1- or HSF1-expression plasmids prior to further treatment. Chromatin fragments from sonicated cells with or without heat shock were taken as input, which were then immunoprecipitated with anti-Flag M2 affinity gel (F1). Aliquots of the F1 chromatin fragments were reverse cross-linked to obtain DNA for qPCR assays or saved for re-immunoprecipitation by a second antibody against phosphorylated Y-701- or S727-Stat1 in reChIP assays (F2). DNA extracted from the ReChIPed chromatin fragments was amplified with the primer sets again in qPCR. The relative amounts of pY- or pS-Stat1 recruited by antibody against Brg1 or HSF1 at 42 °C were quantified relative to those recruited at 37 °C and set to an arbitrary value of 1.

*Quantitative real-time RT-PCR analysis*

Total RNA extracted from cells was subjected to reverse transcription in 1st-strand RT-PCR kit (Promega) followed by qPCR analysis as described above. The relative mRNA expression level of each detected genes is normalized against *gapdh* . Primer pairs for each detected genes are listed in Supplementary information, Table S5.

*Restriction endonuclease accessibility analysis*

Jurkat cells and Raji cells were treated with heat shock for 1 h or with IFNγ for 12 h. A total of $1 \times 10^7$ cells were washed twice in PBS and once in NE buffer (20 mM HEPES pH 7.9, 50 mM KCl, 0.5% NP-40) and were incubated on ice for 30 min. Nuclei were spun at 800× *g* for 2 min at 4 °C, and suspended in restriction enzyme buffer (Takara), combined with 15 U of *Apa*I, *Pst*I or *Sac*I (Takara), and digested at 37 °C for 15 min. DNA was extracted for qPCR by using primers given in Supplementary information, Table S6.

## References

1   de la Serna IL, Ohkawa Y, Imbalzano AN. Chromatin remodelling in mammalian differentiation: lessons from ATP-dependent remodellers. *Nat Rev* 2006; **7**:461-473.

2   Flaus A, Owen-Hughes T. Mechanisms for ATP-dependent chromatin remodelling: farewell to the tuna-can octamer? *Curr Opin Genet Dev* 2004; **14**:165-173.

3   Klochendler-Yeivin A, Muchardt C, Yaniv M. SWI/SNF chromatin remodeling and cancer. *Curr Opin Genet Dev* 2002; **12**:73-79.

4   Mohrmann L, Verrijzer CP. Composition and functional specificity of SWI2/SNF2 class chromatin remodeling complexes. *Biochim Biophys Acta* 2005; **1681**:59-73.

5   Chi T. A BAF-centred view of the immune system. *Nat Rev Immunol* 2004; **4**:965-977.

6   Martens JA, Winston F. Recent advances in understanding chromatin remodeling by Swi/Snf complexes. *Curr Opin Genet Dev* 2003; **13**:136-142.

7   Flowers S, Nagl NG, Jr, Beck GR, Jr, Moran E. Antagonistic roles for BRM and BRG1 SWI/SNF complexes in differentiation. *J Biol Chem* 2009; **284**:10067-10075.

8   Nagl NG, Jr, Wang X, Patsialou A, Van Scoy M, Moran E. Distinct mammalian SWI/SNF chromatin remodeling complexes with opposing roles in cell-cycle control. *EMBO J* 2007; **26**:752-763.

9   Strobeck MW, Reisman DN, Gunawardena RW, *et al.* Compensation of BRG-1 function by Brm: insight into the role of the core SWI-SNF subunits in retinoblastoma tumor suppressor signaling. *J Biol Chem* 2002; **277**:4782-4789.

10  Kadam S, Emerson BM. Transcriptional specificity of human SWI/SNF BRG1 and BRM chromatin remodeling complexes. *Mol Cell* 2003; **11**:377-389.

11  Muchardt C, Yaniv M. When the SWI/SNF complex remodels...the cell cycle. *Oncogene* 2001; **20**:3067-3075.

12  Bultman S, Gebuhr T, Yee D, *et al.* A Brg1 null mutation in

the mouse reveals functional differences among mammalian SWI/SNF complexes. *Mol Cell* 2000; **6**:1287-1295.

13 Bultman SJ, Gebuhr TC, Magnuson T. A Brg1 mutation that uncouples ATPase activity from chromatin remodeling reveals an essential role for SWI/SNF-related complexes in beta-globin expression and erythroid development. *Genes Dev* 2005; **19**:2849-2861.

14 Wu JI, Lessard J, Crabtree GR. Understanding the words of chromatin regulation. *Cell* 2009; **136**:200-206.

15 Lessard J, Wu JI, Ranish JA, *et al.* An essential switch in sub-unit composition of a chromatin remodeling complex during neural development. *Neuron* 2007; **55**:201-215.

16 Cheng MB, Zhang Y, Zhong X, *et al.* Stat1 mediates an auto-regulation of *hsp90beta* gene in heat shock response. *Cell Signal* 2010; **22**:1206-1213.

17 Levy DE, Darnell JE, Jr. Stats: transcriptional control and biological impact. *Nat Rev Mol Cell Biol* 2002; **3**:651-662.

18 Platanias LC. Mechanisms of type-I- and type-II-interferon-mediated signalling. *Nat Rev Immunol* 2005; **5**:375-386.

19 Schindler C, Levy DE, Decker T. JAK-STAT signaling: from interferons to cytokines. *J Biol Chem* 2007; **282**:20059-20063.

20 Chen XS, Zhang Y, Wang JS, *et al.* Diverse effects of Stat1 on the regulation of *hsp90alpha* gene under heat shock. *J Cell Biochem* 2007; **102**:1059-1066.

21 Giraud S, Hurlstone A, Avril S, Coqueret O. Implication of BRG1 and cdk9 in the STAT3-mediated activation of the *p21waf1* gene. *Oncogene* 2004; **23**:7391-7398.

22 Huang M, Qian F, Hu Y, *et al.* Chromatin-remodelling factor BRG1 selectively activates a subset of interferon-alpha-inducible genes. *Nat Cell Biol* 2002; **4**:774-781.

23 Bourachot B, Yaniv M, Muchardt C. Growth inhibition by the mammalian SWI-SNF subunit Brm is regulated by acetylation. *EMBO J* 2003; **22**:6505-6515.

24 Holling TM, Schooten E, Langerak AW, van den Elsen PJ. Regulation of MHC class II expression in human T-cell malignancies. *Blood* 2004; **103**:1438-1444.

25 Yoo AS, Crabtree GR. ATP-dependent chromatin remodeling in neural development. *Curr Opin Neurobiol* 2009; **19**:120-126.

26 Wu JM, Xiao L, Cheng XK, *et al.* PKC epsilon is a unique regulator for *hsp90 beta* gene in heat shock response. *J Biol Chem* 2003; **278**:51143-51149.

27 Mao X, Ren Z, Parker GN, *et al.* Structural bases of unphosphorylated STAT1 association and receptor binding. *Mol Cell* 2005; **17**:761-771.

28 Yang J, Stark GR. Roles of unphosphorylated STATs in signaling. *Cell Res* 2008; **18**:443-451.

29 Sullivan EK, Weirich CS, Guyon JR, Sif S, Kingston RE. Transcriptional activation domains of human heat shock factor 1 recruit human SWI/SNF. *Mol Cell Biol* 2001; **21**:5826-

5837.

30 Qing Y, Stark GR. Alternative activation of STAT1 and STAT3 in response to interferon-gamma. *J Biol Chem* 2004; **279**:41679-41685.

31 Calo V, Migliavacca M, Bazan V, *et al.* STAT proteins: from normal control of cellular events to tumorigenesis. *J Cell Physiol* 2003; **197**:157-168.

32 Laherty CD, Yang WM, Sun JM, *et al.* Histone deacetylases associated with the mSin3 corepressor mediate mad transcriptional repression. *Cell* 1997; **89**:349-356.

33 Silverstein RA, Ekwall K. Sin3: a flexible regulator of global gene expression and genome stability. *Curr Genet* 2005; **47**:1-17.

34 van Oevelen C, Wang J, Asp P, *et al.* A role for mammalian Sin3 in permanent gene silencing. *Mol Cell* 2008; **32**:359-370.

35 Hassan AH, Neely KE, Workman JL. Histone acetyltransferase complexes stabilize swi/snf binding to promoter nucleosomes. *Cell* 2001; **104**:817-827.

36 Gresh L, Bourachot B, Reimann A, *et al.* The SWI/SNF chromatin-remodeling complex subunit SNF5 is essential for hepatocyte differentiation. *EMBO J* 2005; **24**:3313-3324.

37 Roberts CW, Galusha SA, McMenamin ME, Fletcher CD, Orkin SH. Haploinsufficiency of Snf5 (integrase interactor 1) predisposes to malignant rhabdoid tumors in mice. *Proc Natl Acad Sci USA* 2000; **97**:13796-13800.

38 Memedula S, Belmont AS. Sequential recruitment of HAT and SWI/SNF components to condensed chromatin by VP16. *Curr Biol* 2003; **13**:241-246.

39 Wang W, Xue Y, Zhou S, *et al.* Diversity and specialization of mammalian SWI/SNF complexes. *Genes Dev* 1996; **10**:2117-2130.

40 Li ZY, Yang J, Gao X, *et al.* Sequential recruitment of PCAF and BRG1 contributes to myogenin activation in 12-O-tetradecanoylphorbol-13-acetate-induced early differentiation of rhabdomyosarcoma-derived cells. *J Biol Chem* 2007; **282**:18872-18878.

41 Xiao L, Lang W. A dominant role for the c-Jun NH2-terminal kinase in oncogenic ras-induced morphologic transformation of human lung carcinoma cells. *Cancer Res* 2000; **60**:400-408.

42 Kuo MH, Allis CD. *In vivo* cross-linking and immunoprecipitation for studying dynamic Protein:DNA associations in a chromatin environment. *Methods* 1999; **19**:425-433.

43 Zhang Y, Wang JS, Chen LL, *et al.* Repression of *hsp90beta* gene by p53 in UV irradiation-induced apoptosis of Jurkat cells. *J Biol Chem* 2004; **279**:42545-42551.

44 Tahiliani M, Mei P, Fang R, *et al.* The histone H3K4 demethylase SMCX links REST target genes to X-linked mental retardation. *Nature* 2007; **447**:601-605.

(**Supplementary information** is linked to the online version of the paper on the *Cell Research* website.)